Journal Club 2010/06/04
鈴木

An excess of star-forming galaxies in the fields of high-redshift QSOs

Stevens et al. 2010

概要
z~2のサブミリ波で明るい5つの QSO 周囲におけるSMG面密度超過の報告。

・QSO周囲でも星形成活動の集中が示唆された
・電波銀河周囲のSMGsよりも星形成活動は弱い傾向であった

背景

SMGが集まっているhigh z原始銀河団領域の指標
＝高密度領域？
＝巨大銀河形成が起こっている？
＝巨大BHが存在する？
＝AGNが存在する？

幾つかの例
・電波銀河(e.g. Ivison et al. 2000; Kurk et al. 2000; Pentericci et al. 2000; Smail et al. 2003; Stevens et al. 2003; De Breuck et al. 2004; Greve et al. 2007; Venemans et al. 2007)
・QSO周囲(Stevens et al. 2004; Priddey, Ivison & Isaak 2008)

=> concentrated on extreme objects, those with the highest luminosities and at the highest redshifts

typical QSOsではどうか？

SMGナンバーカウント、星形成活動を電波銀河やextreme QSOsと比較。

サンプル

- 1.7 < z < 2.8のサブミリ波で明るいQSO
- Hard X ray selected QSOs
- 計5天体領域

Table 1. The sample of QSOs mapped with SCUBA.

Name	RA (J2000.0)	Dec. (J2000.0)	z	$\log(L_X)$ [log (erg s^{-1})]	$\log(L_{FIR})$ [log ($L_\odot$)]
RX J005734.78−272827.4	$00^h57^m34^s.94$	−27°28′28″.0	2.19	$44.85^{+0.14}_{-0.14}$	$13.32^{+0.08}_{-0.06}$
RX J094144.51+385434.8	$09^h41^m44^s.61$	+38°54′39″.1	1.82	$44.83^{+0.12}_{-0.14}$	$13.41^{+0.05}_{-0.07}$
RX J121803.82+470854.6	$12^h18^m04^s.54$	+47°08′51″.0	1.74	$44.69^{+0.17}_{-0.15}$	$13.10^{+0.08}_{-0.10}$
RX J124913.86−055906.2	$12^h49^m13^s.85$	−05°59′19″.4	2.21	$45.10^{+0.10}_{-0.13}$	$13.11^{+0.09}_{-0.11}$
RX J163308.57+570258.7	$16^h33^m08^s.59$	+57°02′54″.8	2.80	$45.24^{+0.11}_{-0.10}$	$13.00^{+0.08}_{-0.11}$

Note. Coordinates are those of the optical QSO. Absorption corrected X-ray luminosities are given for the 0.5–2 keV band whilst FIR luminosities are calculated from submm photometric observations at 850 μm (see Stevens et al. 2005 for more details on how these luminosities were calculated).

観測

- SCUBA/JCMT 450 & 850 um
  - 64 point Jiggle mapping 2波長同時観測
  - 各々~5arcmin^2、計28.4arcmin^2
- Spitzer IRAC 4.5 & 8.0 um/ MIPS 24 um

Table 3. Observing log of the *Spitzer* observations.

Name	IRAC 4.5/8.0 μm		MIPS 24 μm	
	Date (yy/mm/dd)	T_{int} (s)	Date (yy/mm/dd)	T_{int} (s)
RX J005734.78−272827.4	2005/07/17	2000	2005/12/02	432
RX J094144.51+385434.8	2005/05/06	3000	2005/04/12	336
RX J121803.82+470854.6	2005/05/06	2000	2005/05/19	210
RX J124913.86−055906.2	2005/07/15	5000	2005/06/27	636
RX J163308.57+570258.7	2005/03/26	1000	2005/03/06	970

Note. For each field, we give the date of observation and the on-source integration time (T_{int}) for each instrument.

結果：カタログ抽出

850 um(SHADESと同じ抽出基準)
- S/N > 2
- > 0mJyの事前確率分布>95%
- 計21天体(QSO 4つ)

450 um
- S/N > 3
- no deboost
- > 0mJyの事前確率分布>95%
- 計14天体(QSO 3つ)

450 & 850 天体
- <10arcsecで一致：8つ(うちQSO3つ)

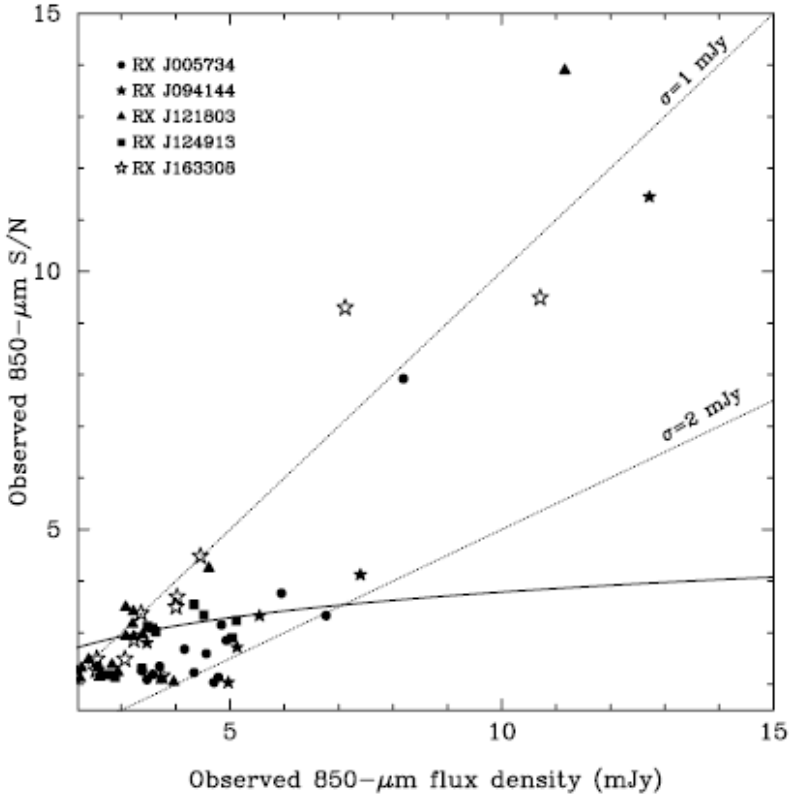

Figure 2. Extracted 850-μm flux density against extracted 850-μm S/N (uncorrected for flux density boosting). All sources extracted with S/N > 2 are plotted; those that fall above the solid line have >95 per cent posterior probability that their flux density is >0 mJy. These sources make it into our catalogue. Dotted lines show noise levels of 1 and 2 mJy beam^{-1}.

結果：ナンバーカウント (850 um)

コンプリートネス補正して評価
表6:QSO含めたもの
表7:QSO除いたもの

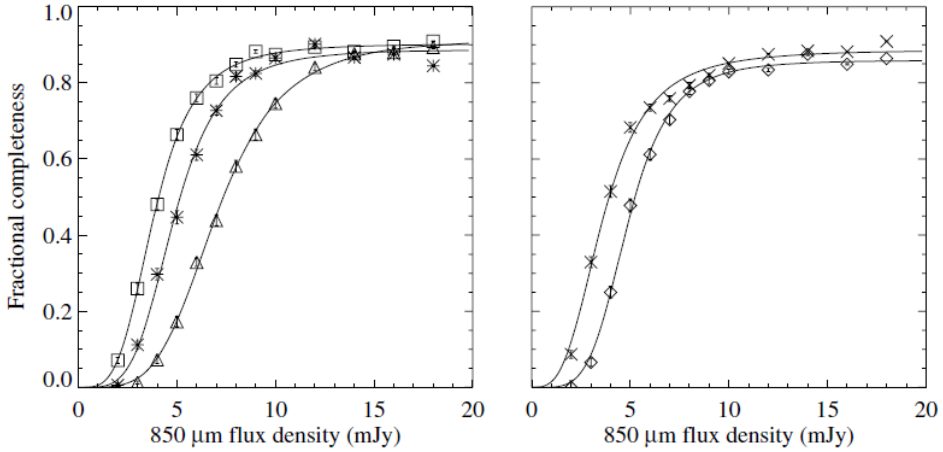

Figure 3. Fractional completeness as a function of 850-μm flux density for each of the five fields. The curves are fits to the data (see text for details). The left-hand panel shows the completeness for RX J163308 (squares), RX J121803 (diamonds) and RX J094144 (triangles) while the right-hand panel shows the completeness for RX J124913 (asterisks) and RX J005734 (diamonds).

Table 6. Combined integral number counts for the five QSO fields including the QSOs.

Flux density (mJy)	850-μm integral counts, $N(>S)$ (deg^{-2})	
	This work	SHADES
2.0	$11\,072^{+6019}_{-2791}$	2506^{+407}_{-407}
4.0	2074^{+1060}_{-470}	844^{+117}_{-117}
6.0	953^{+507}_{-305}	362^{+61}_{-59}
8.0	552^{+278}_{-258}	150^{+35}_{-35}
10.0	375^{+190}_{-237}	68^{+21}_{-21}
12.0	120^{+85}_{-105}	33^{+16}_{-15}

Note. Bins are quoted at the lower flux density bound. The bins are of width 2 mJy. SHADES counts are taken from Coppin et al. (2006).

Table 7. Combined integral number counts for the five QSO fields excluding the QSOs.

Flux density (mJy)	850-μm integral counts, $N(>S)$ (deg^{-2}) This work
2.0	$10\,420^{+3676}_{-3584}$
3.0	3574^{+1129}_{-1211}
4.0	1423^{+524}_{-540}
5.0	636^{+308}_{-300}
6.0	343^{+205}_{-190}
7.0	227^{+156}_{-167}
8.0	175^{+146}_{-151}
9.0	139^{+130}_{-131}

Note. Bins are quoted at the lower flux density bound. The bins are of width 1 mJy.

結果：ナンバーカウント(850 um)

SHADES(点線)との比較

・< 4mJyでSHADESに比べ超過。

・＞4mJyではSHADESとコンシステント。

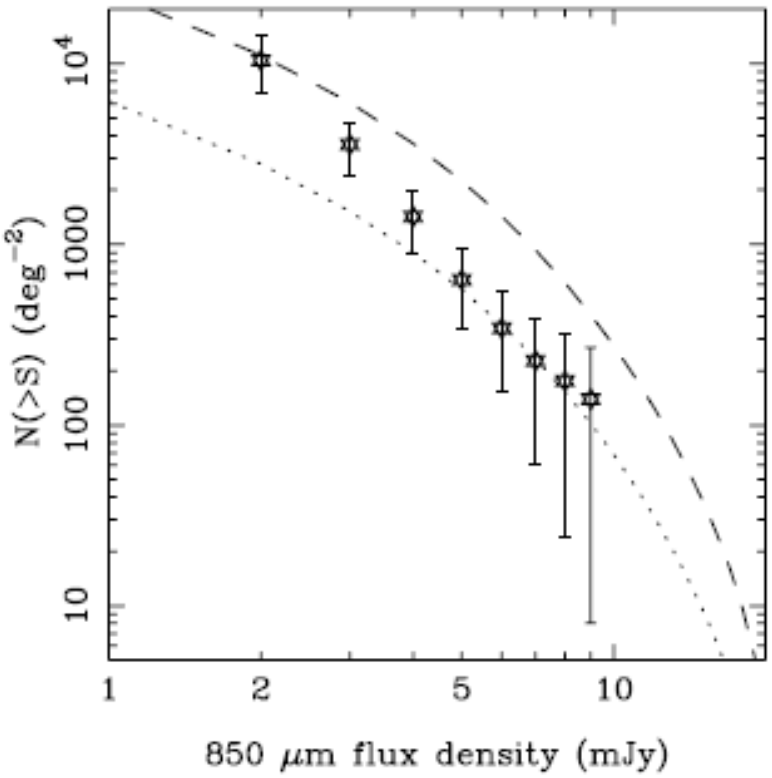

Figure 4. Integral number counts plotted in 1 mJy bins. The QSOs have been removed from the counts. The dotted line is a best-fitting Schechter function to the SHADES counts as described in Coppin et al. (2006) while the dashed line is the result of multiplying this fit by 4 and is shown for reference.

結果：MIRカウンターパートと色

・全てのQSO、6割のSMGのMIRカウンターパート同定。
・QSOsはAGNライク(非熱的パワーロー)な色
・SMGsはULIRGライク(星成分、dust/PAH)な色

図の線は、Arp220(AGN host)とMrk231,NGC6240(ULIRG)の色進化

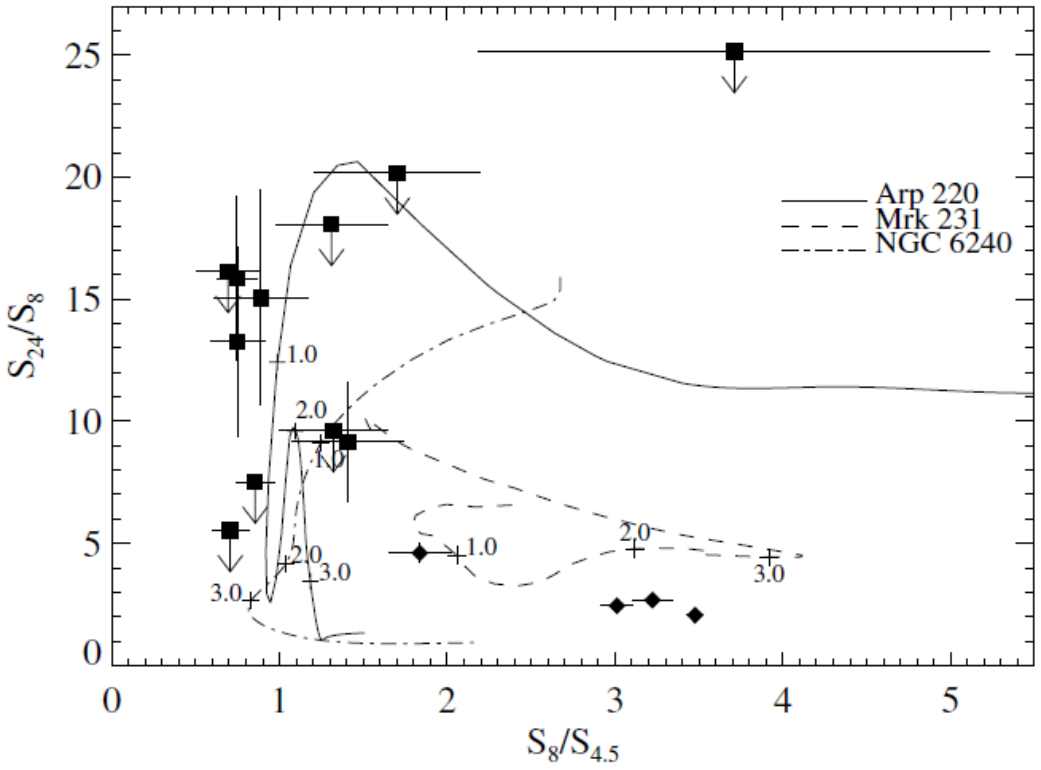

Figure 5. Colour–colour plot for those sources detected in two or three of the observed *Spitzer* bands (24, 8.0 and 4.5 μm). The QSOs are plotted as diamonds while the submm-selected galaxies discovered in their fields are shown as squares. Lines show the redshifted colour tracks of three local ultraluminous infrared galaxies (ULIRGs) with (Mrk 231) and without (Arp 220 and NGC 6240) obvious signatures of powerful AGNs at MIR wavelengths. Redshifts of 1.0, 2.0 and 3.0 are marked on each of these tracks.

議論: 星形成率

・850 um SMGsのflux distribution 3-10mJy
・星形成率 400-1300 Msun / yr

z>3のサンプル(Stevens +2003)との比較
・2つのextremely bright(S(850um) > 20mJy)@z>3
⇔今回のサンプルのほうが低い星形成率である傾向。

結論

・サブミリで明るいTypical QSOsでもblank fieldに比べ、< 4mJy でoverdensityが見られた。
・統計的には言えないが、Low z, low powerful, radio quiet なAGN周囲のSMGは
low SFRの傾向。

Jiggle mappingの概念図(Holland+ 1999)

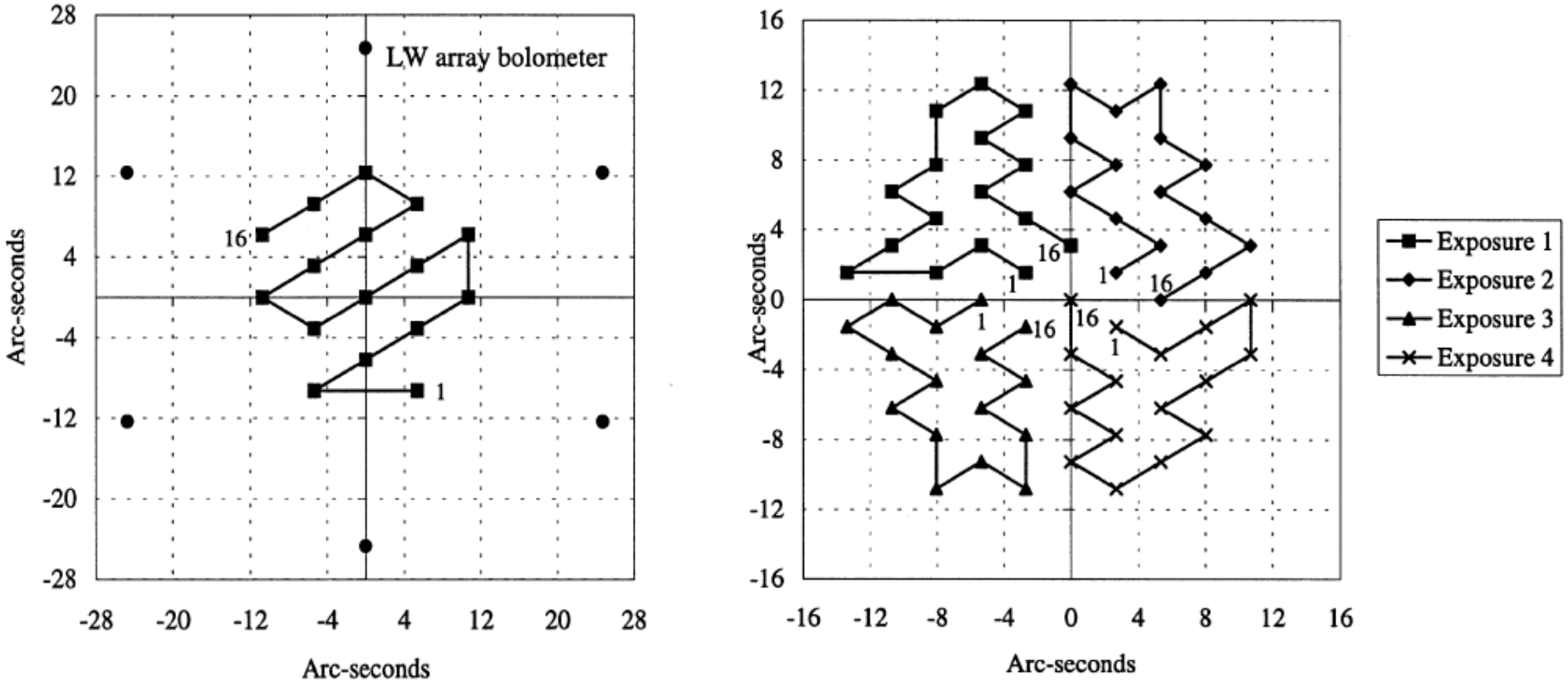

Figure 4. (a) Jiggle pattern to fully sample the LW array alone. (b) Jiggle pattern to fully sample both arrays simultaneously.

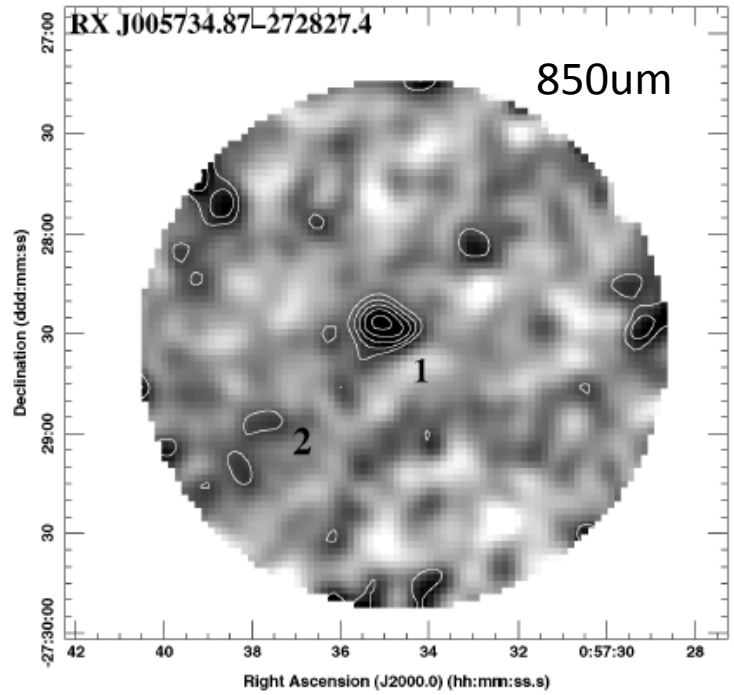
RX J005734.87–272827.4
850um
1
2
Declination (ddd:mm:ss)
Right Ascension (J2000.0) (hh:mm:ss.s)

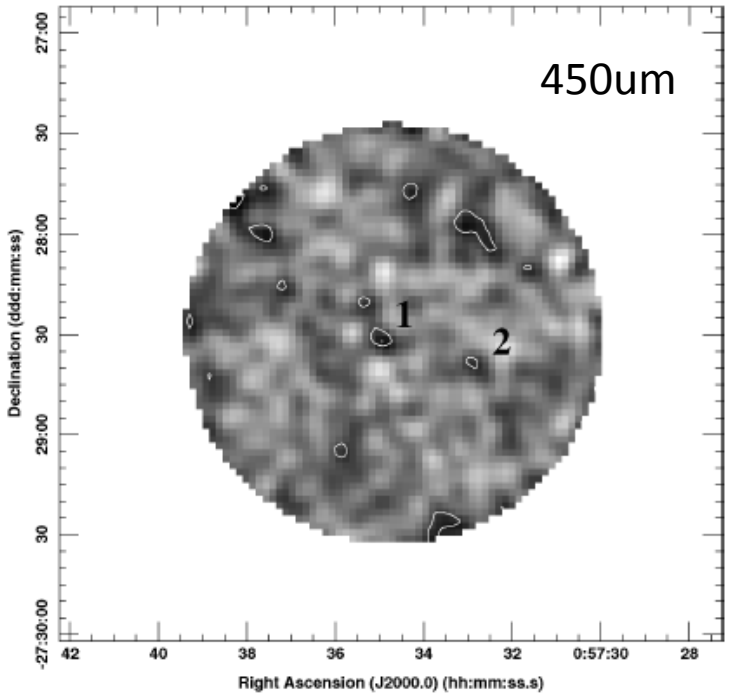
450um
1
2
Declination (ddd:mm:ss)
Right Ascension (J2000.0) (hh:mm:ss.s)

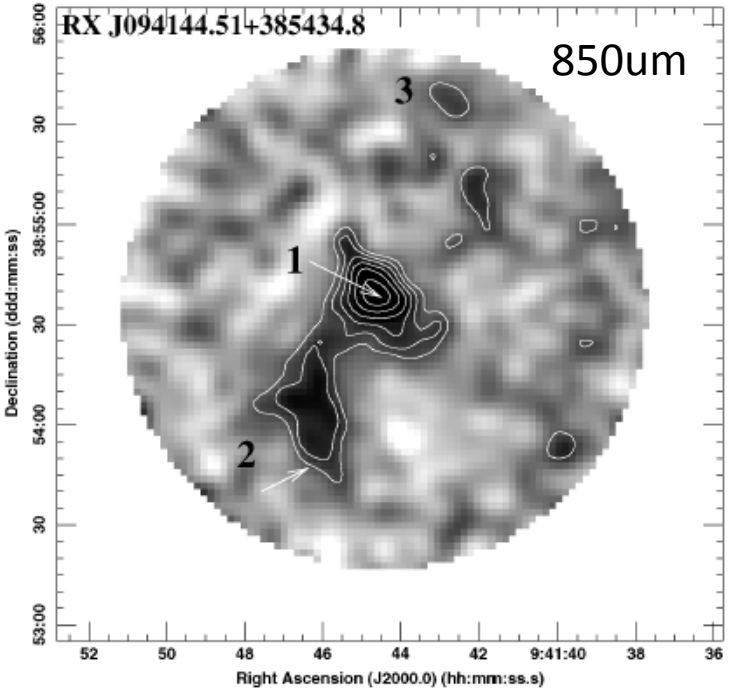
RX J094144.51+385434.8
850um
1
2
3
Declination (ddd:mm:ss)
Right Ascension (J2000.0) (hh:mm:ss.s)

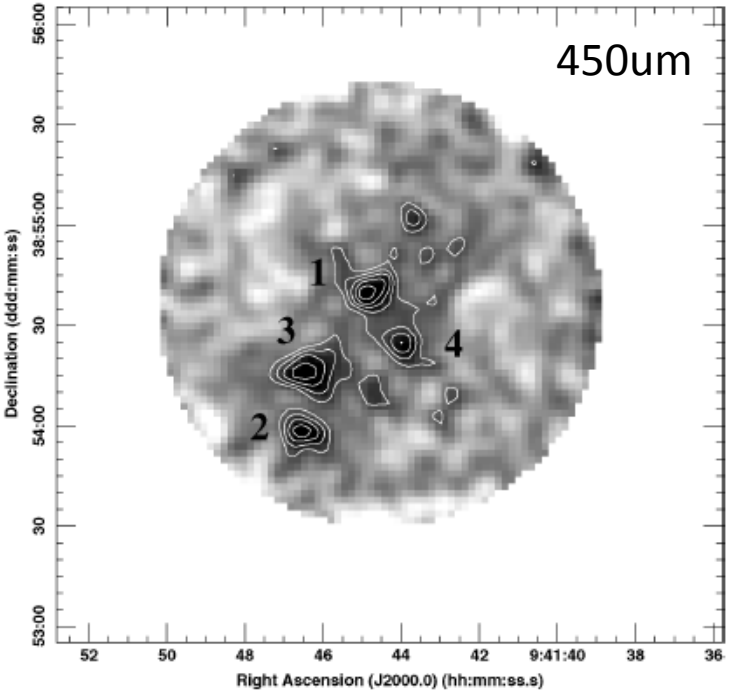
450um
1
2
3
4
Declination (ddd:mm:ss)
Right Ascension (J2000.0) (hh:mm:ss.s)

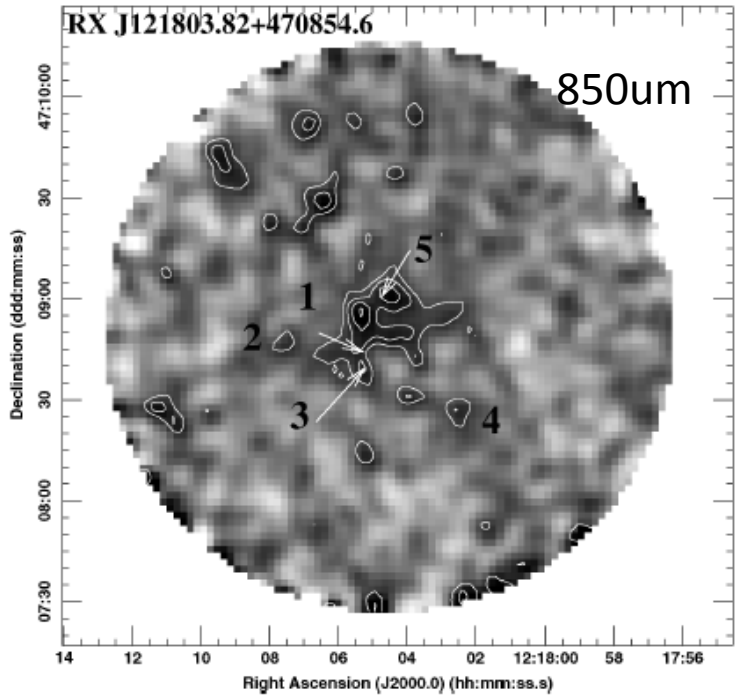
RX J121803.82+470854.6
850um
Declination (ddd:mm:ss)
Right Ascension (J2000.0) (hh:mm:ss.s)

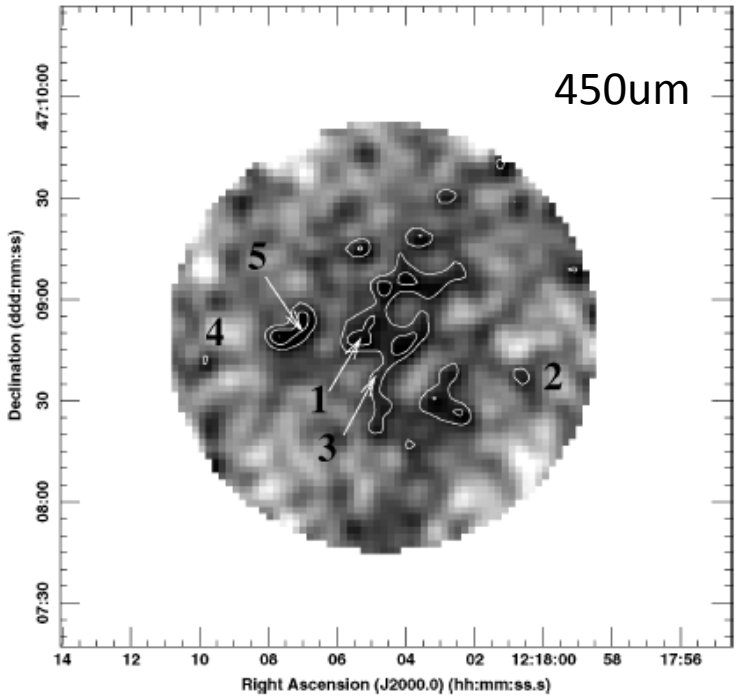
450um
Declination (ddd:mm:ss)
Right Ascension (J2000.0) (hh:mm:ss.s)

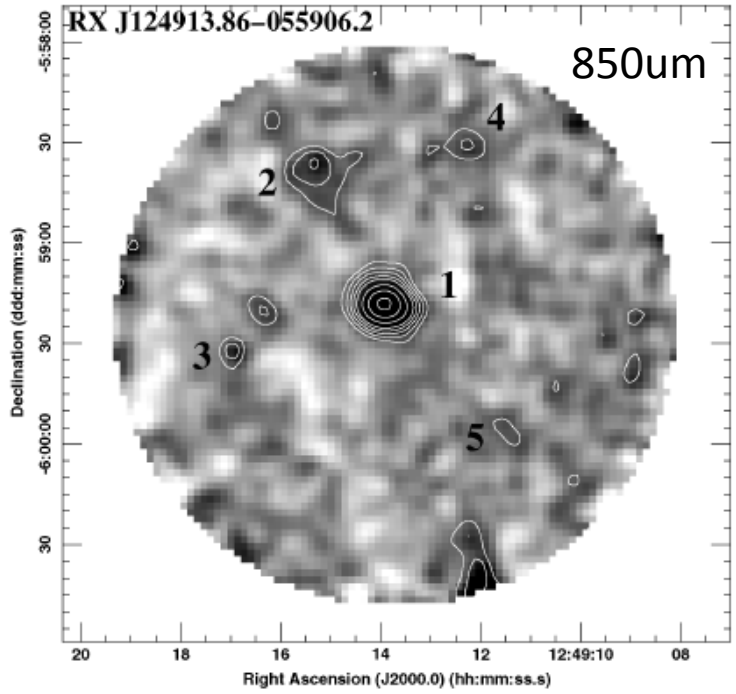
RX J124913.86−055906.2
850um
Declination (ddd:mm:ss)
Right Ascension (J2000.0) (hh:mm:ss.s)

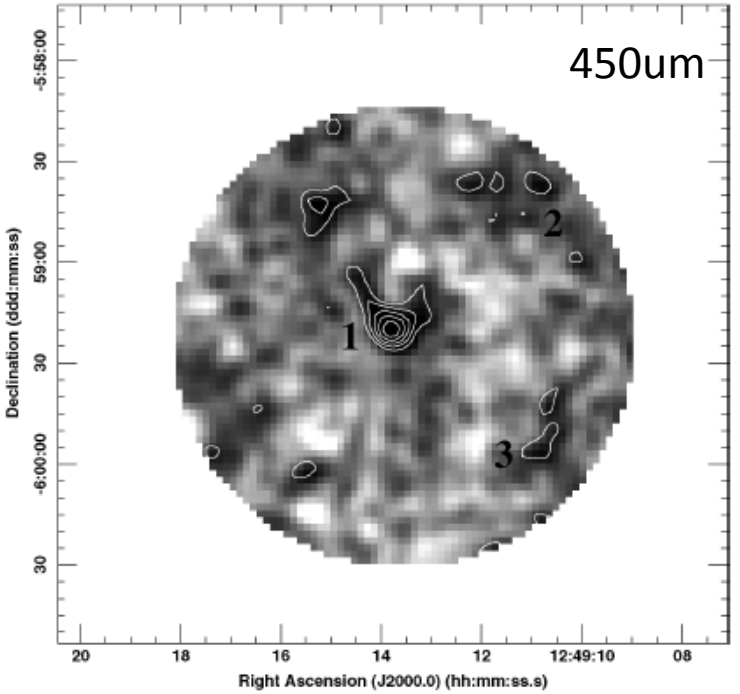
450um
Declination (ddd:mm:ss)
Right Ascension (J2000.0) (hh:mm:ss.s)

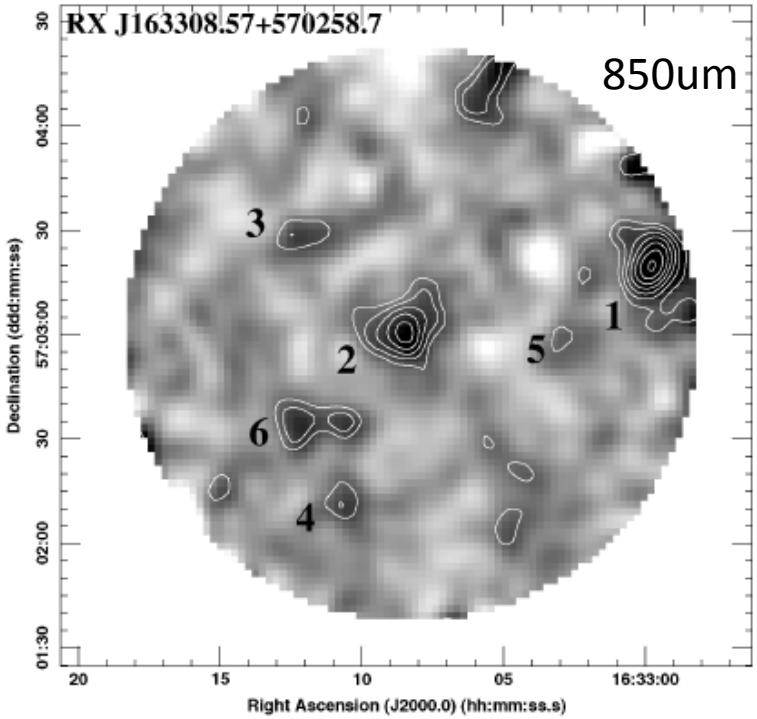
RX J163308.57+570258.7
850um
3
2
1
5
6
4
Declination (ddd:mm:ss)
Right Ascension (J2000.0) (hh:mm:ss.s)
30
04:00
57:03:00
30
02:00
01:30
20
15
10
05
16:33:00

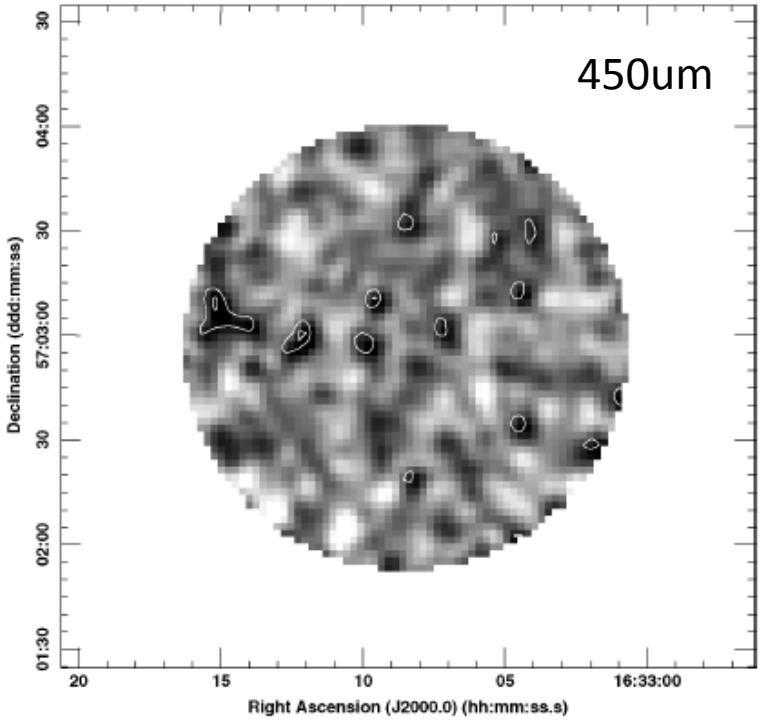
450um
Declination (ddd:mm:ss)
Right Ascension (J2000.0) (hh:mm:ss.s)
30
04:00
57:03:00
30
02:00
01:30
20
15
10
05
16:33:00

Table 4. The 850-μm catalogue.

Field	ID#	RA (J2000.0)	Dec. (J2000.0)	S_{850} (mJy beam^{-1})	S_{850} (deb.) (mJy beam^{-1})	Map S/N	Note
RX J005734.78−272827.4	1	$00^h57^m35^s.21$	$-27°28'27''.9$	8.2 ± 1.2	$7.8^{+1.0}_{-0.9}$	7.9	QSO
	2	$00^h57^m37^s.79$	$-27°28'57''.9$	5.9 ± 1.6	$4.3^{+1.7}_{-2.1}$	3.8	
RX J094144.51+385434.8	1	$09^h41^m44^s.84$	$+38°54'36''.9$	12.7 ± 1.4	$12.4^{+1.1}_{-1.0}$	11.4	QSO
	2	$09^h41^m46^s.53$	$+38°53'54''.7$	7.4 ± 1.9	$5.7^{+2.0}_{-2.1}$	4.1	
	3	$09^h41^m42^s.80$	$+38°55'34''.8$	5.5 ± 1.7	$3.1^{+2.1}_{-2.2}$	3.3	
RX J121803.82+470854.6	1	$12^h18^m05^s.51$	$+47°08'55''.1$	4.3 ± 1.3	$3.1^{+1.3}_{-1.6}$	3.5	
	2	$12^h18^m07^s.66$	$+47°08'45''.1$	4.5 ± 1.4	$2.8^{+1.6}_{-1.7}$	3.3	
	3	$12^h18^m05^s.53$	$+47°08'36''.9$	3.6 ± 1.2	$2.1^{+1.3}_{-1.3}$	3.1	
	4	$12^h18^m02^s.76$	$+47°08'24''.9$	3.5 ± 1.2	$2.1^{+1.3}_{-1.2}$	3.1	
	5	$12^h18^m04^s.74$	$+47°08'59''.0$	3.6 ± 1.2	$1.9^{+1.5}_{-1.2}$	3.0	
RX J124913.86−055906.2	1	$12^h49^m13^s.99$	$-05°59'19''.3$	11.2 ± 1.1	$11.0^{+0.7}_{-0.7}$	13.9	QSO
	2	$12^h49^m15^s.45$	$-05°58'37''.3$	4.6 ± 1.1	$3.8^{+1.1}_{-1.1}$	4.3	
	3	$12^h49^m17^s.06$	$-05°59'33''.3$	3.1 ± 0.9	$2.3^{+0.9}_{-1.0}$	3.5	
	4	$12^h49^m12^s.37$	$-05°58'33''.5$	3.2 ± 1.0	$2.3^{+1.0}_{-1.0}$	3.4	
	5	$12^h49^m11^s.56$	$-05°59'59''.3$	3.2 ± 1.0	$2.1^{+1.1}_{-1.1}$	3.2	
RX J163308.57+570258.7	1	$16^h32^m59^s.99$	$+57°03'18''.7$	10.7 ± 1.4	$10.4^{+1.0}_{-1.1}$	9.5	
	2	$16^h33^m08^s.82$	$+57°02'58''.7$	7.1 ± 0.9	$6.9^{+0.7}_{-0.7}$	9.3	QSO
	3	$16^h33^m12^s.74$	$+57°03'26''.7$	4.5 ± 1.0	$3.8^{+1.0}_{-1.0}$	4.5	
	4	$16^h33^m10^s.78$	$+57°02'10''.7$	4.0 ± 1.1	$3.0^{+1.2}_{-1.3}$	3.7	
	5	$16^h33^m03^s.18$	$+57°02'58''.7$	4.0 ± 1.2	$2.8^{+1.3}_{-1.4}$	3.5	
	6	$16^h33^m12^s.61$	$+57°02'32''.0$	3.4 ± 1.1	$2.3^{+1.1}_{-1.1}$	3.4	

Note. Coordinates give the extracted position of the source. Also listed are extracted flux density and S/N together with deboosted flux density (see text for details). Quoted uncertainties on the raw flux densities include contributions from the calibration uncertainty and the extracted S/N values while those on the deboosted flux densities are purely statistical.

Table 5. The 450-μm catalogue.

Field	ID#	RA (J2000.0)	Dec. (J2000.0)	S_{450} (mJy beam^{-1})	Map S/N	Note
RX J005734.78−272827.4	1	$00^h57^m35^s.08$	$-27°28'34''.1$	32.4 ± 10.2	4.1	QSO
	2	$00^h57^m33^s.13$	$-27°28'40''.1$	25.9 ± 9.6	3.2	
RX J094144.51+385434.8	1	$09^h41^m45^s.06$	$+38°54'36''.7$	44.7 ± 10.2	9.1	QSO
	2	$09^h41^m46^s.73$	$+38°53'56''.7$	41.2 ± 10.0	7.3	850#2
	3	$09^h41^m46^s.73$	$+38°54'14''.9$	33.5 ± 8.8	5.9	
	4	$09^h41^m44^s.16$	$+38°54'22''.7$	28.8 ± 7.8	5.5	
RX J121803.82+470854.6	1	$12^h18^m05^s.51$	$+47°08'47''.1$	35.1 ± 8.9	6.4	850#1
	2	$12^h18^m00^s.80$	$+47°08'34''.9$	31.9 ± 10.7	3.7	
	3	$12^h18^m05^s.11$	$+47°08'35''.1$	30.4 ± 11.0	3.3	850#3
	4	$12^h18^m10^s.02$	$+47°08'41''.1$	24.3 ± 8.8	3.3	
	5	$12^h18^m07^s.08$	$+47°08'52''.9$	21.9 ± 8.3	3.1	850#2
RX J124913.86-055906.2	1	$12^h49^m13^s.97$	$-05°59'21''.3$	34.9 ± 8.1	8.7	QSO
	2	$12^h49^m11^s.03$	$-05°58'37''.5$	21.6 ± 7.7	3.4	
	3	$12^h49^m11^s.03$	$-05°59'57''.5$	33.7 ± 12.5	3.2	850#5

Note. Coordinates give the extracted position of the source. Also listed are extracted flux density and S/N. Quoted uncertainties on the raw flux densities include contributions from the calibration uncertainty and the extracted S/N values. The last column gives the likely ID if the 450-μm position falls within 10 arcsec of either the QSO or one of the objects extracted at 850 μm.